Secondary Voltage Regulation Based on Full-State Feedback - Performance Assessment with Dynaωo

Tom Vancorsellis*, Julien Callec*, Carmen Cardozo*, Philippe Juston* and Sami Tliba†
* R&D - System Stability
RTE, La Defense, France
julien.callec@rte-france.com
† Laboratoire des Signaux et Systèmes
Université Paris-Saclay–CNRS–CentraleSupélec, Gif-sur-Yvette, France

***Abstract*—This paper discusses the performance assessment of new secondary voltage regulators currently under study in France to address challenges posed by the energy transition. With renewable integration and increasing cross-border interconnections, power flow variations surge across the network. Coupled with the historical SVRs' relatively slow response, operational since the late 1970s, recent observations show higher voltage volatility. Prior research has already highlighted the potential of two novel regulators: the *Average Q*-SVR and the *LQ*-SVR, in mitigating these issues. Our focus here centres on the latter and begins by discussing the implications of control design hypotheses on closed-loop system performance. These include linearisation, neglecting communication delays, and assuming uniform dynamic behaviour across all resources. We then propose a two-step control design, leveraging Linear Quadratic Regulator (LQR) and eigenstructure placement methods and demonstrate that this approach surpasses the LQR method alone in terms of transient reactive power tracking.**

***Index Terms*—Voltage control, System modeling, System dynamics, Full-state feedback, Linear quadratic regulator.**

I. Introduction

Voltage regulation is an important task for Transmission System Operators (TSOs) to ensure a proper trade-off between efficiency, power system quality, and security. High voltage profiles are desirable for losses reduction and power transfer capability maximisation. At the same time, the voltage must be maintained within acceptable ranges at all buses and at all times to prevent the premature ageing of equipment and avoid potential misoperation of protection systems. To achieve this goal, a combination of distributed and centralised strategies is typically implemented, involving both automatic and manual actions. Historically, Synchronous Generators (SGs) have been equipped with a local Automatic Voltage Regulator (AVR), while TSOs have deployed dedicated assets, either passive (such as capacitor or reactor banks) or active (synchronous condensers or Flexible AC Systems (FACTS) such as Static VAR Compensator (SVC) or StatComs), as necessary.

However, as we progress in the energy transition and market integration, the voltage control strategies currently in place may become poorly suited to accommodate the ongoing modifications of the power system topology and operational practices [1]. The main factors driving these changes include:

1) New assets are often connected using underground cables, accentuating the capacitive nature of the grid.
2) Distributed generation displaces conventional units, thereby reducing the availability of voltage regulation service providers at the High Voltage (HV) level. Additionally, it tends to decrease power flow on the HV network, thereby reducing reactive power losses.
3) The increasing variability of power flow, resulting from both renewable integration and the development of cross-border interconnections, may lead to a growing volatility of the voltage, as depicted in Fig. 1. Spikes often observed at rounded hours are correlated with market-driven rescheduling of active power. In this particular case, the situation is exacerbated by the active and reactive power coupling of a nearby Line Commutated Converter (LCC) High Voltage Direct Current (HVDC) link and the slow dynamics of the French Secondary Voltage Regulator (SVR).

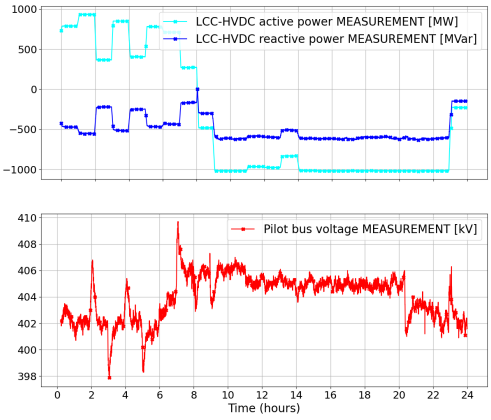

Fig. 1: Measurements of the active and reactive power output of the LCC - HVDC (top) and 400 kV nearby bus (bottom)

The first two points result in a shortfall of regulating capacity, mainly inductive, which has been partially addressed by requiring voltage regulation capabilities for Power Electronic Interfaced Resources (PEIR) in Connection Network Codes (CNC) [2], along with the installation of inductors [3].

Submitted to the 23rd Power Systems Computation Conference (PSCC 2024).

The last point concerns the degradation of voltage control dynamic performance, particularly regarding the SVR and its ability to counteract active power flow fluctuations. Historically, only a few countries, including Italy and France, have considered it necessary to deploy SVR [1]. More recently, HOPS, the Croatian TSO, addressed the voltage regulation problem in the Sincro.Grid Volt Var Control (VVC) EU funded project [4], proposing actions on reactive power injections and transformers' On-Load Tap Changers (OLTC) [4]. Similarly, *Red Eléctrica de España (REE)*, the Spanish TSO, designed a new automatic scheme, VOLTAIREE, incorporating Optimized Voltage Regulation (OVR) on top of the SVR [5]. More generally, recent works on voltage control tend to focus on optimizing pilot bus voltage references, known as the Tertiary Voltage Regulator (TVR), or directly optimizing the AVR references [6]. The latter may be particularly relevant in microgrid applications or for automaton design in sub-transmission networks, where more measurements are available and state estimation migth not be required. Exploring the economic aspects of service provision has also drawn attention [1]. However, these topics lie beyond the scope of this work.

Latest developments on the French SVR have been published in [7], [8], and will be briefly recalled in Sections II and IV. Additionally, a redesign of the Italian SVR also using the LQR approach has been recently proposed [9]. However, this work primarily focused on the selection of the controller input states from a practical viewpoint, based on the available measures. Moreover, the control performance was validated using a simplified simulation model. Finally, the study does not provide a discussion on the computation of the controller gains or the expected performance limitations when deviating from the design hypotheses. To fill these gaps, this work proposes an in-depth discussion on the simplification hypotheses applied to the open-loop system model for control design purposes and the consequence they have on its dynamic response. Special attention is given to the diversity, in terms of dynamics, of the different regulating resources (SGs and PEIR) and the presence of high communication delays. Indeed, French SVR relies on the industrial Supervisory Control And Data Acquisition (SCADA) system which currently has a sampling period of 10 s, while [9] considers Phasor Measurement Unit (PMU) data. Moreover, developed Modelica models will be made publicly available. Finally, a two step control design procedure is proposed: the LQR method is used for optimal pole placement, but the final gains are obtained by eigenstructure placement to achieve a specific coupling between modes and states, which in practice yield to a transient alignment of reactive power between the different resources.

The remainder of this paper is organised as follows: Section II begins by providing background on the principles of voltage control in France. Next, Section III highlights the differences between the control design and simulation system models. Section IV recalls the various SVR control laws under investigation, offering a thoughtful discussion on their tuning. Simulation results are presented in Section V and conclusions are drawn in Section VI.

II. Voltage regulation in France

Since the late 1970s, voltage regulation in France relies on cascaded primary and secondary automatic controls [10]. The former is achieved by an AVR implemented in most power generation units to regulate their terminal voltage within a few seconds. The reference signals of these local controllers are updated in real time by a distributed SVR. In practice, each SVR regulates the voltage of a specific bus $\mathbf{v}_p(t)$, called the *pilot bus*, by computing a per unit level, $Lz(t)$, which reflects the need for reactive power modulation in each control zone. Then, a Reactive Power Control Loop (RPCL), historically present in most conventional power plants, computes individual AVR references from the level given by the SVR. New power plants such as Combined Cycle Gas Turbine (CCGT) and PEIR, including FACTS, may receive directly a voltage reference for the AVR.

A. Voltage regulation priciple

Fig. 2 illustrates this principle if we consider that:

- the system output variable y is the scalar $\mathbf{v}_p(t)$, and
- the control variables **u1** and **u2** are, respectively, the per unit reactive power levels **L**, for the units with a local RPCL, and $\mathbf{v}_{ref}$, for units receiving voltage references.

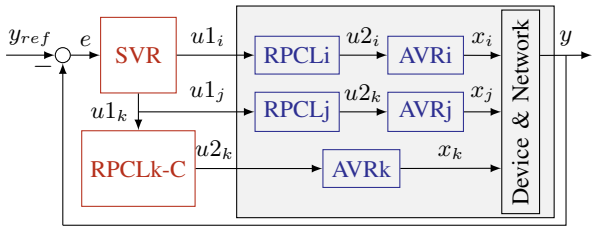

Fig. 2: SVR principle diagram

By implementing a RPCL in the control centre (RPCL-C) for the units controlled in voltage, and setting $u1_i = u1_j = u1_k = Lz(t)$, a Single Input Single Output (SISO) system is obtained. In this framework, a SVR can be easily designed using simple Proportional-Integral (PI) controllers, provided that the network topology allows the system to be split into electrically independent zones (see Section II-C for details).

B. Revisiting the SVR control law

This solution has proved to be effective in a system dominated by centralised and dispatchable generation, typically based on SGs, and has the advantage of requiring limited access to IT information. However, the current SISO PI-based SVR exhibits a relatively slow response, which is becoming an issue considering larger and faster voltage variations.

- On the one hand, the cascaded structure restricts the dynamics of the SVR which is set to be slower than the RPCL. Moreover, the currently implemented SVR suffers from a non-minimum phase behaviour that tends to slow down the voltage recovery following disturbances [7].

- On the other hand, network reinforcements may increase the coupling of zones that were considered nearly independent [11]. This could potentially lead to oscillations when attempting to accelerate the current SVR.

To overcome those limitations while taking advantage of the availability of additional real-time measurements, RTE, the French TSO, is revisiting the SVR control. This work led to the design of two new regulators currently under study:

1) The *Average Q*-SVR including real-time measurement of the reactive power outputs of the units [8].
2) The *LQ*-SVR: a full-state feedback controller, without a RPCL-C, based on the formulation of the SVR as a Multiple-Input Multiple-Output (MIMO) problem [7].

Prior research in [7] was mainly focused on revisiting the SVR control objectives and ensuring their feasibility, which led to the design of a multi variable PI controller. Optimal gains were computed based on the LQR theory considering current SVR response time. Preliminary results exhibited promising performance and robustness with respect to grid parameter uncertainties, communication delays and disturbance rejection. However, the RPCL model was initially neglected and the regulating units were considered identical. Validation was performed with Eurostag (RTE transient stability tool), hence using fairly detailed dynamic models; but this tool is poorly suited to assess the new SVR impact on key system wide stability indicators (in the relevant frequency range). In this work, validation is performed through time-domain simulations using Dynaωo, the open-source hybrid Modelica/C++ suite of simulation tools [12], paving the way for voltage stability assessment.

C. Control zones and pilot points

In general, pilot buses are selected based on their short-circuit power, while the allocation of resources to specific control zones is determined by sensitivity coefficients that represent the impact of unit reactive power variation on the pilot bus voltage. In France, the main pilot buses typically correspond to the high-voltage buses of large power plants, which currently form 44 control zones, with half of them located in the 400 kV network and the remaining 22 in the 225 kV network. Terna, the Italian TSO, described an iterative procedure to compute sensitivity coefficients in [13] resulting in less than 20 pilot points. REE proposed a methodology based on the Multi-Infeed Interaction Factor (MIIF) to define zones of electrical influence in the design of a reactive power zonal market, relying on PSS/E power flow simulations [5].

The optimal definition of pilot buses has been the subject of research [14]; however, such methods are not yet implemented in practice. At least in France, each time a new regulating unit is connected to the grid, local teams decide, based on operational criteria and tools, whether the new facility should be added to an existing zone or if a new control zone needs to be created. REE intends to implement one SVR per point of interconnection between the service provider and the transmission network [5]. However, there is a risk that the multiplication of zones could amplify the risk of interactions highlighted in Section II-B. Concerning on-line control zone reconfiguration, RTE, designates backup pilot points in some cases to address measurement issues, while Terna's SVR system appears to allow for switching certain boundary plants from one pilot point to another [15].

III. System modelling

The system open-loop model, highlighted in the grey Fig. 2, includes the generating units with their local control loops (RPCL and AVR) and the network. All modules can be built with different levels of detail. In particular, non-linear simulation models are typically used for time-domain stability analysis and can provide validation references for more simplified models. For instance, when designing a linear feedback control law, linearising the system is a way to study its local stability and use appropriate methods of control design such as the LQR. To limit complexity, it is common practice to also neglect some dynamics that are much faster or slower than the phenomena of interest. Accordingly, in this work, we consider three different versions of the system model:

- the non-linear simulation model - used in DynaWaltz, the voltage stability simulation tool of Dynaωo's suite.
- the linearised model - a linearised version of the DynaWaltz model around a predefined operational point.
- the simplified model - a simplified version of the previous linearisation.

A. Non-linear simulation model

The network is fully represented by the power flow equations (classical phasor approximation). The Synchronous Machines (SM) is modelled as for classic transient stability studies (6th order model). Current injectors are used for PEIR. Regarding the local controllers, the RPCL is represented by a PI controller that regulates the generator reactive power output at its terminal $\mathbf{q}_{s_i}(t)$ to a level dependent reference given by $\mathbf{q}_{s_{ref,i}}(t) = L_i(t)\,\mathbf{q}_{r_i}(t)$, where $\mathbf{q}_{r_i}(t)$ is the unit i participation factor and reflects its maximum capacity in reactive power injection or absorption at a given time. The AVR is also modelled by a PI controller that regulates to the set point $\mathbf{v}_{ref,i}(t)$, given by the RPCL: the unit terminal voltage ($\mathbf{v}_{s_i}(t)$ for SM), or the quantity $\mathbf{v}_{pcc_i} + \lambda\mathbf{q}_{pcc_i}$ at the Point of Common Coupling (PCC) (for PEIR). Input and output limits are considered in both cases, while ramp limitations and dead-bands might be present in some RPCL models. Finally, communication delays are also represented[1].

Generically, such a model is written as a nonlinear state space model where the state variables include the internal variables of the unit (SM for instance), the PI integrators' state variables from the AVR and RPCL, and the measurement

[1]In practice, SVR is a discrete controller located at the control centre, while the simulation models are continuous. In this work, the SCADA sampling period is considered by adding a 10 s Zero-Order Hold (ZOH) at both the system input and output to account for delays at the command sending and measurement arrival. In addition, a 5 s additional delay accounts for Digital-to-Analog Converter (DAC) leading to a 25 s closed-loop nominal delay.

filters, while the system's control inputs are the reactive power level ($\mathbf{L}$) and/or voltage references ($\mathbf{v}_{ref}$).

B. Linearised model

All non-linearities are removed from the previous DynaWaltz model:

- first, the electrical part (network and devices) is linearised using sensitivity matrices that link some network variables - the voltage of the pilot bus $\mathbf{v}_p(t)$ (rather variations of the voltage from the operational point) - and the units' reactive powers $\mathbf{q}_{s_i}(t)$ to the voltages $\mathbf{v}_{s_i}(t)$, with:

$$\mathbf{v}_p(t) = \mathbf{C}_v\,\mathbf{v}_s(t), \tag{1}$$
$$\mathbf{q}_s(t) = \mathbf{C}_q\,\mathbf{v}_s(t), \tag{2}$$

  where the matrices $\mathbf{C}_v$ and $\mathbf{C}_q$ can be obtained by different methods. In this work, we simulate small variation of $\mathbf{v}_{s_i}$ $\forall i = 1, 2, \ldots, N$ at the vicinity of the operating point, with the RPCL in open-loop, using an instance of the full network non-linear system. Note that i is the unit number and N the total amount of regulating resources, including $\tilde{N} \leq N$ units of SM-type and $\check{N} = N - \tilde{N}$ of PEIR-type (controlled in voltage, without local RPCL).
- Then, the dead-band and ramp limitation in the RPCL are removed (or set to zero and high value, respectively).
- Finally, *Padé approximation* is used to linearise delays.

C. Simplified model for control design

In order to keep only the state variables that can be measured, the following simplifications are added to the previous linearised model:

- the AVR dynamics are neglected and replaced by a unitary static gain. Indeed, those dynamics (<10s) can be considered fast compared to the RPCL ones (1-2 minutes). Hence, $\mathbf{v}_s = \mathbf{v}_{s_{ref}}$ which is the output of the RPCL and naturally becomes the state vector:

$$\dot{\mathbf{v}}_{s_i} = \frac{1}{ti_{Q_i}}(\mathbf{q}_{s_{ref,i}} - \mathbf{q}_{s_i}) = \frac{1}{ti_{Q_i}}(\mathbf{q}_{r_i} N_i - \mathbf{C}_{q_i}\mathbf{v}_s), \tag{3}$$

  with $\mathbf{C}_{q_i}$ standing for the i^{th} row of the matrix $\mathbf{C}_q$.
- the delays are also replaced by unitary static gains.

The simplified model can be put into the following state-space equation:

$$\dot{\mathbf{v}}_s = \mathbf{A}\,\mathbf{v}_s + \mathbf{B}\,\mathbf{u}, \quad \mathbf{v}_s(0) := \mathbf{v}_{s0}, \tag{4}$$
$$\text{with} \quad \mathbf{v}_s = \begin{bmatrix}\mathbf{v}_{s_1} & \mathbf{v}_{s_2} & \mathbf{v}_{s_3} & \mathbf{v}_{s_4} & \mathbf{v}_{s_{PV}}\end{bmatrix}^T, \tag{5}$$
$$\mathbf{u} = \begin{bmatrix}u_1 & u_2 & u_3 & u_4 & u_{PV}\end{bmatrix}^T, \tag{6}$$

for a system with four SM and one Photovoltaic (PV) power plant, as described in paragraph V-A and considered in the sequel, where u_i, $i = 1 \ldots 4$, are the reactive power level references, u_{PV} is the voltage reference at PCC and $\mathbf{v}_{s0}$ is the initial state vector. Matrix $\mathbf{A}$ and $\mathbf{B}$ are provided in Appendix A. As they are also monitored, the reactive power outputs of the generators, $\mathbf{q}_{s_i}$, could also be considered as the state variables instead of the variables $\mathbf{v}_{s_i}$.

D. Model validation

Figs. 3a and 3b show respectively the reactive power and terminal voltage of SM 1 (in solid lines) when submitted to a reactive power level step (N_1, at 10 s). In dashed lines we include the SM 2 response, whose RPCL sees the step as a disturbance. We observe that both, the linearised and simplified models are able to accurately reproduce the steady-state response of the reference model for small variations around the point of linearisation, including at the pilot bus (see Fig. 3c). The RPCL overall dynamic (rise time[2]) can also be properly approximated. In addition, we illustrate that Padé approximations allow for the incorporation of delays in a linear manner, albeit at the cost of introducing spurious oscillations at the beginning of the response. Finally, the system reaction to disturbances is adequately captured by the simplified model as it is dominated by the RPCL dynamics.

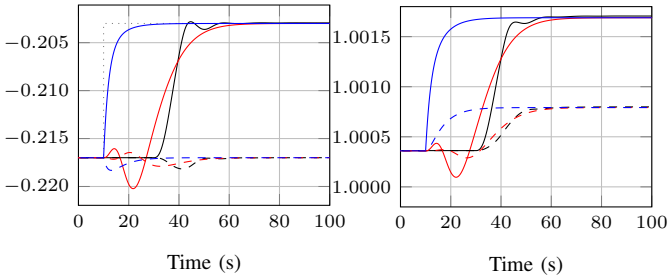

(a) Reactive power ($\mathbf{q}_{s_i}$ [pu]) (b) Terminal voltage ($\mathbf{v}_{s_i}$ [pu])

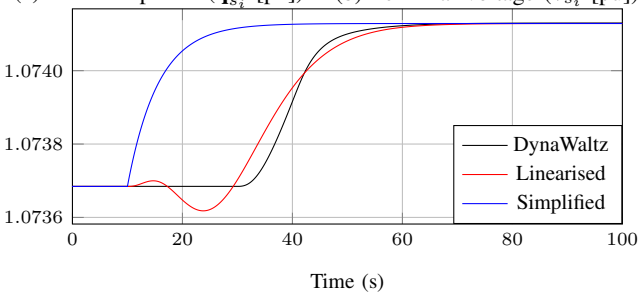

(c) Pilot bus voltage ($\mathbf{v}_p$ [pu])

Fig. 3: Open-loop dynamic response - N_1 step

IV. Secondary Voltage Regulators

A. Control objectives

As recalled in [7] and [8], SVR control objectives can be summarised as follows:

1) ensure zero static tracking error on the voltage of the pilot bus within a predefined response time (typically 3-10 minutes) and limited overshoot (aperiodic response is desirable),
2) reject asymptotically the constant disturbances that may happen at the inputs of the system[3],

[2]According to IEC 61400-21, defined as the difference between the time the response reaches 90% of the target value, and the reaction time, i.e. when it reaches 10% of the target value (delays are then disregarded).

[3]Variations on the operational conditions such as changes in the topology, active, reactive power injections and flows; load, generation and compensation devices connection/disconnection; and changes in the poll of regulating units.

3) no interaction with cascaded local controls (RPCL) or neighbouring SVR,
4) share control effort among regulating units proportionally to their capacity[4] (reactive power alignment, during transient desirable),
5) be robustness to measurement noise and increased delays due to temporally communication loss (at least 3 sampling periods, i.e. +30 s).
6) Ensure proper anti-windup behaviour when regulating resources reach capability limits.

Available data includes:

1) the pilot bus voltage,
2) voltage, active and reactive power at the resource terminal, and
3) binary signals indicating that the regulating unit has reached output limitations (indicating its direction: upwards or downwards).

Additional functionalities requested in operation include the possibility to apply an off-set ($\mathbf{q}_{os_i}$) or limitation to the reactive power output ($\mathbf{q}_{max_i}$, $\mathbf{q}_{min_i}$) of individual units.

The units traditionally participating in SVR are the SGs connected at the 400 kV and 225 kV levels, but large PV and wind farms are now signing agreements with RTE to provide this service. In the future, transmission connected loads using IGBT based converters such as some electrolyzers, datacenters, as well as batteries, could participate in SVR. The impact of the contribution of distribution systems to transmission system voltage regulation will be assessed in prospective studies to determine if a coordinate regulation would be beneficial.

B. Control laws

1) SISO PI-SVR (in operation): as aforementioned, the currently implemented French SVR is based on a PI controller that regulates the voltage of the pilot bus ($\mathbf{v}_p(t)$) to a user-defined reference value $\mathbf{v}_{p_{ref}}(t)$, as given in (7) where α and β are the controller gains. In practice, the unit i level is given by (8), considering the possible user-defined offset.

$$\begin{aligned} Lz(t) = &\beta(vp_{ref}(t) - v_p(t)) \\ &+ \alpha \int_0^T (vp_{ref}(t) - v_p(t))dt. \end{aligned} \tag{7}$$

$$L_i(t) = Lz(t) + \frac{\mathbf{q}_{os_i}(t)}{\mathbf{q}_{r_i}(t)}. \tag{8}$$

2) Average Q-SVR: the zone level for the Average Q-SVR is given by (9) [8]:

$$Lz(t) = \beta(v_{p_{ref}}(t) - v_p(t)) + L_{ave}, \tag{9}$$

where $L_{ave} = \dfrac{\sum \mathbf{q}_{s_i}(t) - \mathbf{q}_{os_i}(t)}{\sum \mathbf{q}_{r_i}(t)}$ is the *average level*.

Analogously, the unit i level is given by (10) considering the level correction and the user-defined offset:

$$L_i(t) = Lz_f(t) + \Delta L_i(t) + \frac{\mathbf{q}_{os_i}(t)}{\mathbf{q}_{r_i}(t)}. \tag{10}$$

[4]Choice historically made by RTE, but other reactive power sharing criteria could be enforced.

Without loss of generality, in the following $\mathbf{q}_{os_i}(t)$ is supposed zero to simplify the notation.

3) Full-state feedback-SVR: as already established in [7], it is possible to build a state feedback control law ensuring zero static tracking error on the pilot bus voltage while asymptotically rejecting constant disturbances additive to the inputs. In that case, an integral action, placed before the disturbance, is required within the control structure. In the state-space formalism, it consists in considering the augmented state (13) and the equivalent state-space equation (11) and then, by designing the state feedback control law (16) for the initial system in (4).

$$\dot{\mathbf{x}}_{aug} = \mathbf{A}_{aug}\,\mathbf{x}_{aug} + \mathbf{B}_{aug}\,\dot{\mathbf{u}}, \tag{11}$$

with

$$\mathbf{e} := \begin{bmatrix} \mathbf{e}_1 & \cdots & \mathbf{e}_{N-1} & \mathbf{e}_N \end{bmatrix}^T, \tag{12}$$

$$\mathbf{x}_{aug} := \begin{bmatrix} \dot{\mathbf{v}}_s & \mathbf{e} \end{bmatrix}^T, \quad \mathbf{x}_{aug} \in \mathbb{R}^{2N}, \tag{13}$$

$$\mathbf{A}_{aug} = \begin{bmatrix} \mathbf{A} & \mathbf{0}_{N\times N} \\ -\begin{bmatrix} \mathbf{G}\mathbf{C}_q \\ \mathbf{C}_v \end{bmatrix} & \mathbf{0}_{N\times N} \end{bmatrix}, \quad \mathbf{B}_{aug} = \begin{bmatrix} \mathbf{B} \\ \mathbf{0}_{N\times N} \end{bmatrix}, \tag{14}$$

$$\mathbf{G} = \begin{bmatrix} diag(q_{r,1}, \cdots, q_{r,\check{N}})^{-1} & \mathbf{0}_{\check{N}\times 1} \end{bmatrix} - \frac{\begin{bmatrix} \mathbf{I}_{\check{N}} & \mathbf{0}_{\check{N}\times 1} \end{bmatrix}}{\sum_{i=1}^{N} q_{r,i}}, \tag{15}$$

where $\check{N} = N - 1$ and the $\mathbf{e}_i$ stands for the errors.

Different choices for the error signals can be considered. According to [7] setting $\mathbf{e}_i := \Delta L_i = L_{ave} - \frac{\mathbf{q}_{s_i}}{\mathbf{q}_{r_i}}$ for $i = 1, \ldots, (N-1)$ and $\mathbf{e}_N := \mathbf{v}_p - \mathbf{v}_{p_{ref}}$, ensures reactive power alignment in addition to pilot bus voltage tracking. Although the theoretical relevance of this approach was demonstrated, in practice, we need to select the Nth unit whose reactive power tracking is *implicitly* achieved. Then, handling the reconfiguration of the SVR as different units join/leave the pool of regulating resources might result cumbersome. Inspired by the Average Q-SVR, we could consider $\mathbf{e}_i = L_{ave} + \beta(\mathbf{v}_p - \mathbf{v}_{p_{ref}}) - \frac{\mathbf{q}_{s_i}}{\mathbf{q}_{r_i}}\ \forall i = 1, \ldots, N$, where β becomes a non-zero parameter that sets the weight of the pilot bus voltage tracking error in these expressions.

In both cases, the state-feedback control law is then:

$$\begin{aligned} \dot{\mathbf{u}} &= -\,\mathbf{K}\,\mathbf{x}_{aug}, \\ \text{giving} \quad \mathbf{u} &= -\,\mathbf{K} \begin{bmatrix} \mathbf{v}_s \\ \int_0^t \mathbf{e}(\tau)\,d\tau \end{bmatrix}, \end{aligned} \tag{16}$$

to be applied to system in (4), where $\mathbf{K} \in \mathbb{R}^{N\times 2N}$ is the sought state-feedback gain matrix.

C. Controller design method

There exist several methods to compute the state feedback gain for a MIMO system having some required closed-loop properties. In our study case (considering $N = 5$ units), such a gain matrix has $2N^2$ degrees of freedom (dofs), whereas only $2N$ among them are required to assign the $2N$ closed-loop poles. There are $2N^2 - 2N$ dofs that can be used to address other control objectives. In particular, dynamic reactive power

alignment can be formulated as the coupling between some the closed-loop modes and state variables in (13). The proposed control design procedure consists then in two steps:

1) First, a state feedback is computed for the augmented system in (11) by the LQR approach [16]. More than the related state-feedback gain itself, the aim is instead to obtain the closed-loop poles that minimise the LQ criterion:

$$J = \int_0^{+\infty} \left({\mathbf{x}_{aug}}^T \mathbf{Q}\, \mathbf{x}_{aug} + \mathbf{u}^T \mathbf{R}\, \mathbf{u} \right) d\tau$$

where $\mathbf{R} = \mathbf{R}^T > 0$, $\mathbf{R} \in \mathbb{R}^{N \times N}$ and $\mathbf{Q} = \mathbf{Q}^T \geq 0$, $\mathbf{Q} \in \mathbb{R}^{2N \times 2N}$ are weighting matrices that allow to set different trade-off between performance and robustness.

2) The second step aims to assign a set of eigenvectors related to the computed closed-loop pole in order to meet coupling specifications on the error signals.

1) Linear Quadratic Regulator: the standard LQR optimization problem is based on minimizing an energetic criterion over an infinite time horizon for the closed-loop system subject to any given initial condition. The weighting matrix $\mathbf{Q}$ allows to manage the relative importance between the different states. Usually, for sakes of simplicity, it is a diagonal matrix when the states have a clear physical meaning. The weighting matrix $\mathbf{R}$ is used to set the relative control effort between each control input, and to set the overall control effort dedicated to the optimal control problem. For the test system described in V-A (where $\tilde{N} = 1$), the trades-off on the closed-loop dynamic between each type of unit are managed by using the following weighting matrices:

$$\mathbf{Q} = \begin{bmatrix} q_{v,SM}\mathbf{I}_{\tilde{N}} & \mathbf{0}_{\tilde{N}\times 1} & \mathbf{0}_{\tilde{N}\times\tilde{N}} & \mathbf{0}_{\tilde{N}\times 1} \\ \mathbf{0}_{1\times\tilde{N}} & q_{v,PV} & \mathbf{0}_{1\times\tilde{N}} & \mathbf{0}_{1\times 1} \\ \mathbf{0}_{\tilde{N}\times\tilde{N}} & \mathbf{0}_{\tilde{N}\times 1} & q_q\mathbf{I}_{\tilde{N}} & \mathbf{0}_{\tilde{N}\times 1} \\ \mathbf{0}_{1\times\tilde{N}} & \mathbf{0}_{1\times 1} & \mathbf{0}_{1\times\tilde{N}} & q_{vp} \end{bmatrix}, \quad (17)$$

$$\mathbf{R} = \begin{bmatrix} r_{SM}\mathbf{I}_{\tilde{N}} & \mathbf{0}_{\tilde{N}\times 1} \\ \mathbf{0}_{1\times\tilde{N}} & r_{PV} \end{bmatrix}, \quad (18)$$

where $q_{v,SM}$ and $q_{v,PV}$ are the weightings of the voltages for the units of SM-type and PV-type respectively in the state vector $\mathbf{x}_{aug}$, q_q and q_{vp} are the weightings of the errors in $\mathbf{x}_{aug}$, while r_{SM} and r_{PV} weights the control effort for each type of these units.

2) Eigenstructure assignment: given the system in (11), the eigenstructure assignment method [17] relies on finding the nullspace of the matrix $\mathcal{Q}(\lambda_i)$ defined by:

$$\mathcal{Q}(\lambda_i) := \begin{bmatrix} \mathbf{A}_{aug} - \lambda_i \mathbf{I}_{2N} & -\mathbf{B}_{aug} \end{bmatrix}, \quad i = 1, \ldots, 2N, \quad (19)$$

where $\mathbf{I}_{2N}$ stands for the identity matrix of size $2N$ and λ_i is a desired eigenvalue in closed-loop. Then, let us define the vector $r_i := \begin{bmatrix} \eta_i \\ \nu_i \end{bmatrix}$, where $\eta_i \in \mathbb{R}^{2N}$ is of the same size than $\mathbf{x}_{aug}$ and the vector $\nu_i \in \mathbb{R}^N$ is of the same size than the control vector $\mathbf{u}$. The vector r_i is admissible when $\mathcal{Q}(\lambda_i)\, r_i = 0$ is verified. In that case, η_i is the eigenvector associated with the desired eigenvalue λ_i to be assigned in closed-loop on the augmented system (11), and ν_i is the corresponding input direction. It allows to create some couplings or uncouplings between the mode i and some state variables. The vector η_i allows to link the eigenmode due to λ_i with the desired components of the state vector $\mathbf{x}_{aug}$. Assuming all the selected η_i are independent, $i = 1, \cdots, 2N$, the state feedback gain $\mathbf{K}$ is given by:

$$\mathbf{K} = \begin{bmatrix} \nu_1 & \cdots & \nu_{2N} \end{bmatrix} \begin{bmatrix} \eta_1 & \cdots & \eta_{2N} \end{bmatrix}^{-1}. \quad (20)$$

This state feedback gain matrix ensures the closed-loop eigenstructure relation $(\mathbf{A}_{aug} - \mathbf{B}_{aug}\, \mathbf{K})\, \eta_i = \lambda_i\, \eta_i$, meaning the desired poles' assignment as well as the desired couplings's achievement. The main issue concerning the choice of the closed-loop poles has been tackled thanks to the previous step.

V. Performance assessment

In the following, we first describe the test case in Section V-A. In Section V-B we assess the SVR performance through time domain simulations based on the simplified model when using proposed control design principle. Then, Section V-C discusses the impact of control settings on the SVR closed-loop performance, characterised by the system response time, while Section V-D comments on the robustness to communication delays. Finally, section V-E presents simulations results on the DynaWaltz reference model.

A. Test case and scenario description

Visible in Fig. 4, the test system consists in four identical SGs and a relatively smaller (about four times) PV power plant. The pilot bus is the 400 kV high voltage side of the SM, while the PEIR is connected in 225 kV, hence having limited influence on the pilot bus voltage when compared to the SM. Parameters are representative of a real system and are therefore confidential.

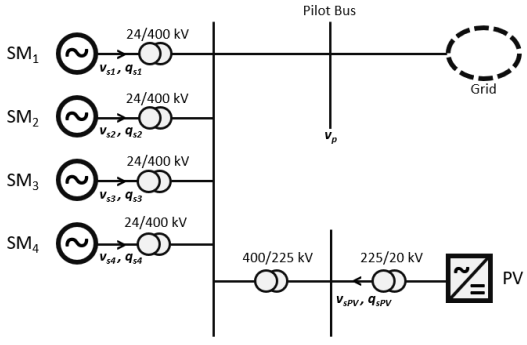

Fig. 4: Test Case single-line diagram

While this work focuses on the control structure, studies are being conducted on a wider system to assess the combined effect of generalising the new controllers to all the control zones of the French electricity network.

B. Time domain simulation with simplified model

Fig. 5 shows the LQ SVR response to a reference step change of -1 kV considering different gain settings:

- Set 1: is obtained by setting $r_{PV} = r_{SM} = 65$, $q_{v,SM} = 0.001$, $q_{v,PV} = 1$, $q_q = 0.1$ and $q_{vp} = 10$.

- Set 2: is obtained by changing $r_{PV} = 10\, r_{SM}$.
- Set 3: is obtained by applying step 2, which means applying an eigenstructure assignment on top of the LQ pole placement, with $\lambda_{vp} = 0.02$ and $\lambda_q = 0.002$.

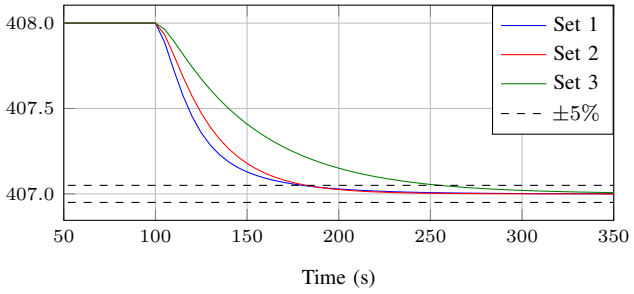

(a) Pilot bus voltage ($\mathbf{v}_p$ [kV])

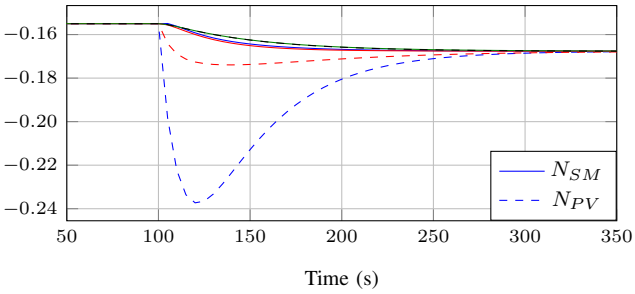

(b) Reactive power ($\mathbf{q}_{s_i}/\mathbf{q}_{r_i}$) [pu]

Fig. 5: -1 kV Step of the pilot bus reference voltage

Fig. 5b shows the normalised reactive power of one of the SM and the PV plant. We can see that depending on the relative value of the **R** matrix elements, the transient response of the reactive power of different resources having specific dynamics may significantly vary (Set 1 vs. Set 2). In this case, this behaviour has low impact on the response time of the pilot point voltage (see Fig. 5a). For the selected settings, a response time of 75 s is reached. Finally, perfect dynamic reactive power alignment (under design hypothesis) can be achieved through eigenstructured assignment (Set 3 in green and dashed black for PV to favour readability). For the specified settings, the obtained response time is 150 s. In general, all else being equal, response time tends to increase with **R** and decreases with q_{vp}.

C. Impacts of delay on performance

Fig. 6 shows the identified response times of the system for a reference step changes, simulating this time the linearised model. For low values of R_0 (or too high values of q_{vp}) the system becomes in fact unstable and high response times correspond to an unacceptable oscillatory behaviour. As illustrated in Fig. 7, settings A and B lead to the same settling time but have different damping (with Set B being of course preferable). Those cases are hereafter disregarded. A minimum ($\approx$ 85 s) appears around $R_0 = 250$ with $R_{PV} > R_{SM}$.

- Set A: is obtained by setting $R_0 = 800$.
- Set B: is obtained by changing $R_0 = 80$.

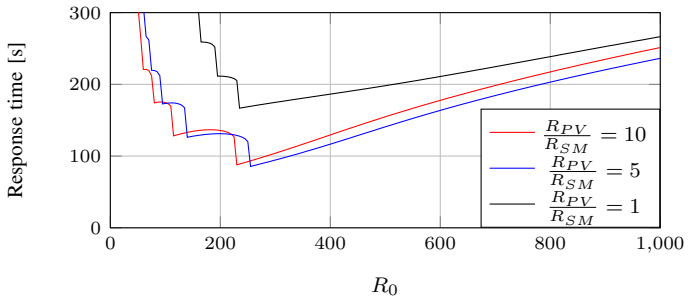

Fig. 6: $\mathbf{v}_p$ Response time as a function of the control settings

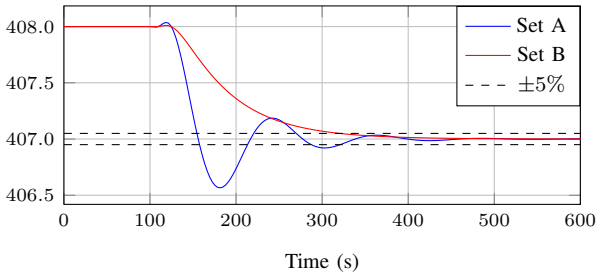

(a) Pilot bus voltage ($\mathbf{v}_p$ [kV])

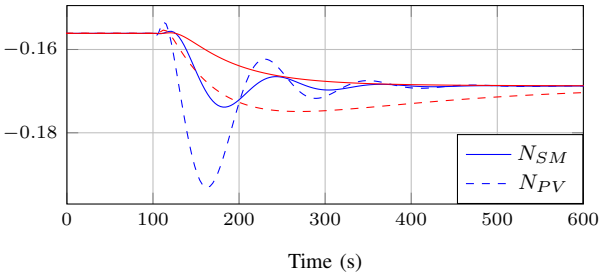

(b) Reactive power ($\mathbf{q}_{s_i}/\mathbf{q}_{r_i}$) [pu]

Fig. 7: -1 kV Step of the pilot bus reference voltage

D. Maximising robustness

As an empirical way to quantify SVR robustness to communication delay we can artificially increase the command transmission delay, simultaneously to all units for simplicity. Interestingly, in Fig. 8 we observe that setting low values q_q increases the delay margin (as defined here) while having low impact on the pilot point voltage response time. However, it will decrease the performance of the transient reactive power tracking, which will be tackled a second stage (step 2).

E. Validation with more accurate models

1) Impact of ramp limits on performance: In Fig. 9 an 8kV $\mathbf{v}_{p_{ref}}$ step has been applied on the DynaWaltz reference model. The ramp limitation on the RPCL of the SM has a clear and visible impact on the pilot bus voltage and its individual level. Without proper handling of the windup phenomena, an overshoot appears. Future work includes the implementation on Modelica and validation of a solution already proposed by the authors of [7].

2) Considering dead-bands in RPCL: The dead-band in the RPCL of the SM Dynawaltz reference model inhibits the SM responses and tends to slow the overall dynamics of the system

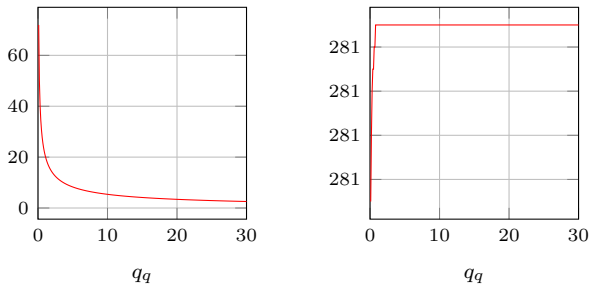

(a) Delay Margin [s] (b) Response Time [s]

Fig. 8: Impact of q_q in robustness and performance

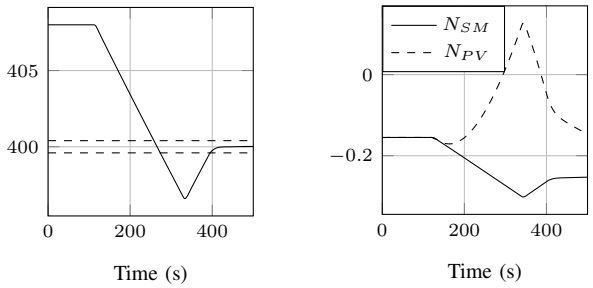

(a) Pilot bus voltage ($\mathbf{v}_p$ [pu]) (b) Reactive power ($\mathbf{q}_{s_i}/\mathbf{q}_{r_i}$) [pu]

Fig. 9: Impact of RPCL ramp limits on the SVR response

(see Fig. 10). At the first instants, only the units with no dead-band, here the PV power plant, take part on the voltage control. As expected, the linear model fails to reproduce the behaviour of the system in such events. Further work is needed to ensure proper response on those cases.

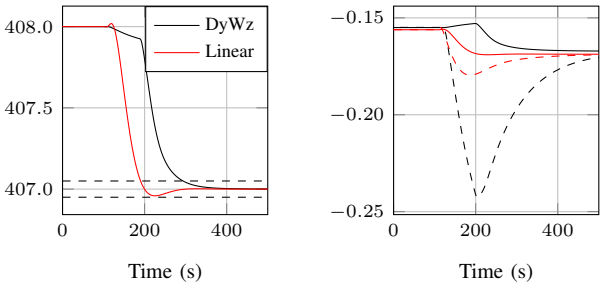

(a) Pilot bus voltage ($\mathbf{v}_p$ [pu]) (b) N_{SM}, N_{PV} [pu]

Fig. 10: Impact of RPCL dead-band on the SVR response

VI. Conclusions

In order to deploy solutions based on advanced control methods, practitioners need to gain confidence in their effectiveness and robustness in real operational environments. In this work, we propose a step forward in increasing the Technological Readiness Level (TRL) of more sophisticated SVR, based on multi-variable PI control. The selected approach is capable of faster tracking of controlled bus voltages while ensuring asymptotic disturbance rejection.

In particular, we have demonstrated the benefits of integral actions and the significance of selecting suitable weighting matrices Q and R to achieve the desired trade-off between closed-loop performance and stability. Furthermore, a noteworthy contribution of this work is the application of the LQR approach, not for direct controller gain calculation, but for optimal pole placement. The latter are used as input for a eigenstructure assignment routine that is able to ensure better transient performance: transient alignment of reactive power, limiting the risk of interactions (oscillations) between different resources. Developed Modelica models will be soon made publicly available on the Dynaω repository.

The response of the LQ-SVR to grid side disturbance is currently under assessment. The simulation results will be included in the final version of the paper, together with a comparison with the SISO PI SVR and the Average-Q SVR in terms of performance, stability and robustness. Moreover, future work will be focused on handling non-linear phenomena such as limitations, with antiwind-up solutions, and reconfiguration when resources join/leave the poll.

Finally, a more advanced control designed directly on the linearised model with an estimation of a part of the state variables is being investigated. Preliminary results indicate the response times below the minimum that appeared in Fig. 6 may be reachable. However, stability and further robustness analysis are still required to confirm these findings.

References

[1] D. Davi-Arderius, M. Troncia, and J. J. Peiró, "Operational challenges and economics in future voltage control services," *Current Sustainable/Renewable Energy Reports*, 2023.

[2] ENTSOE, "Network code on requirements for grid connection of generators," 2016. [Online]. Available: http://data.europa.eu/eli/reg/2016/631/oj

[3] RTE, "Reliability report," 2022. [Online]. Available: https://assets.rte-france.com/prod/public/2023-07/2023-07-18-reliability-report-2022.pdf

[4] R. Rubesa, Z. Buncec, M. Rekic, and T. Stupic, "Practical experience of using fully automated centralized voltage regulation in transmission system," *CIGRE, Paris*, 2022.

[5] J. J. Peiró, J. L. Presa, and M. Caballero, "New voltage control service and voltairee project," 2022.

[6] L. Ortmann, J. Maeght, P. Panciatici, F. Dörfler, and S. Bolognani, "Online feedback optimization for subtransmission grid control," 2023.

[7] A. E. M. Bouzid, B. Marinescu, and G. Denis, "Structural analysis and improved reactive power alignment for secondary voltage control," in *2019 IEEE Milan PowerTech*, 2019, pp. 1–6.

[8] M. Monnet, C. Cardozo, P. Juston, Q. Cossart, and J. Callec, "Revisiting the french secondary voltage regulation and assessing its dynamic behavior with dynaωo," in *2023 IEEE Belgrade PowerTech*, 2023, pp. 1–6.

[9] A. Vicenzutti, F. Marzolla, G. Sulligoi, G. M. Giannuzzi, and C. Pisani, "Study on the state feedback selection and measurement for the application of an lqri secondary voltage regulator to a transmission system," in *2022 20th International Conference on Harmonics & Quality of Power (ICHQP)*, 2022, pp. 1–6.

[10] J. P. Paul, J. Y. Leost, and J. M. Tesseron, "Survey of the secondary voltage control in france : Present realization and investigations," *IEEE Transactions on Power Systems*, vol. 2, no. 2, pp. 505–511, 1987.

[11] H. Lefebvre, D. Fragnier, J. Boussion, P. Mallet, and M. Bulot, "Secondary coordinated voltage control system: feedback of edf," in *2000 Power Engineering Society Summer Meeting (Cat. No.00CH37134)*, vol. 1, 2000, pp. 290–295 vol. 1.

[12] A. Guironnet, M. Saugier, S. Petitrenaud, F. Xavier, and P. Panciatici, "Towards an Open-Source Solution using Modelica for Time-Domain Simulation of Power Systems," in *2018 IEEE PES Innovative Smart Grid Technologies Conference Europe (ISGT-Europe)*, 2018, pp. 1–6.

[13] S. Corsi, M. Pozzi, C. Sabelli, and A. Serrani, "The coordinated automatic voltage control of the italian transmission grid-part i: reasons of the choice and overview of the consolidated hierarchical system," *IEEE Transactions on Power Systems*, vol. 19, no. 4, pp. 1723–1732, 2004.

[14] G. Grigoras, B.-C. Neagu, F. Scarlatache, and R. C. Ciobanu, "Identification of pilot nodes for secondary voltage control using k-means clustering algorithm," in *2017 IEEE 26th International Symposium on Industrial Electronics (ISIE)*, 2017, pp. 106–110.

[15] S. Corsi, M. Pozzi, M. Sforna, and G. Dell'Olio, "The coordinated automatic voltage control of the italian transmission grid-part ii: control apparatuses and field performance of the consolidated hierarchical system," *IEEE Transactions on Power Systems*, vol. 19, no. 4, pp. 1733–1741, 2004.

[16] B. Anderson and J. Moore, *Optimal Control: Linear Quadratic Methods*, ser. Prentice-Hall Int. Series in Optoelectronics. Prentice Hall, 1990.

[17] J. Magni, *Robust Modal Control with a Toolbox for Use with MATLAB®: With a Toolbox for Use With Matlab*. Springer London, Limited, 2002.

APPENDIX A
MODELLING

$$\mathbf{A} = -\begin{bmatrix} \frac{1}{T_{iQ}} & \frac{C_{q12}}{T_{iQ}C_{q11}} & \frac{C_{q13}}{T_{iQ}C_{q11}} & \frac{C_{q14}}{T_{iQ}C_{q11}} & \frac{C_{q14}}{T_{iQ}C_{q15}} \\ \frac{C_{q21}}{T_{iQ}C_{q22}} & \frac{1}{T_{iQ}} & \frac{C_{q23}}{T_{iQ}C_{q22}} & \frac{C_{q24}}{T_{iQ}C_{q22}} & \frac{C_{q25}}{T_{iQ}C_{q22}} \\ \frac{C_{q31}}{T_{iQ}C_{q33}} & \frac{C_{q32}}{T_{iQ}C_{q33}} & \frac{1}{T_{iQ}} & \frac{C_{q34}}{T_{iQ}C_{q33}} & \frac{C_{q35}}{T_{iQ}C_{q33}} \\ \frac{C_{q41}}{T_{iQ}C_{q44}} & \frac{C_{q42}}{T_{iQ}C_{q44}} & \frac{C_{q43}}{T_{iQ}C_{q44}} & \frac{1}{T_{iQ}} & \frac{C_{q45}}{T_{iQ}C_{q44}} \\ \frac{k_I\lambda C_{q51}}{C_{q55}} & \frac{k_I\lambda C_{q52}}{C_{q55}} & \frac{k_I\lambda C_{q53}}{C_{q55}} & \frac{k_I\lambda C_{q54}}{C_{q55}} & \frac{1}{T_{ENR}} \end{bmatrix}, \tag{21}$$

$$\mathbf{B} = \begin{bmatrix} \frac{q_{r,1}}{C_{q11}T_{iQ}} & 0 & 0 & 0 & 0 \\ 0 & \frac{q_{r,2}}{C_{q22}T_{iQ}} & 0 & 0 & 0 \\ 0 & 0 & \frac{q_{r,3}}{C_{q33}T_{iQ}} & 0 & 0 \\ 0 & 0 & 0 & \frac{q_{r,4}}{C_{q44}T_{iQ}} & 0 \\ 0 & 0 & 0 & 0 & \frac{k_I q_{r,ENR}}{C_{q,55}} \end{bmatrix}.$$